The role of posterior parietal cortex in detecting changes in feedback contingency

Sébastien Hélie (`shelie@purdue.edu`)
Department of Psychological Sciences, Purdue University, West Lafayette, IN, USA

Well–practiced or learned behaviors are extremely resilient. For example, it is extremely difficult for a trained typist to forget how to use a keyboard configuration that they are familiar with. While they can be trained on a new keyboard configuration, the original skill quickly comes back when the old keyboard configuration is used again. This resiliency of learned skills is both a blessing and a curse. It makes useful skills durable, but it also makes maladaptive behaviors difficult to extinguish. Crossley, Ashby, and Maddox (2013) proposed a computational model and behavioral paradigm aimed at *unlearning* skills using various feedback contingency manipulations during an extinction phase. They showed that partially—valid feedback during extinction removed evidence for fast reacquisition, which they interpreted as evidence for unlearning. In this article, we replicated the Crossley et al. paradigm using fMRI. Univariate analyses showed differences in BOLD signals between the different experiment phases in the frontoparietal attention network. The superior and inferior parietal lobules (SPL and IPL, respectively) showed the largest cluster differences both between experimental phases and between extinction conditions. In contrast, the prefrontal cortex only showed differences in cluster of activities between extinction conditions. Multivariate pattern analysis was also used with seeds in the SPL and IPL. The results showed that these brain areas were critical in detecting changes in experimental phases. Overall, the fMRI results found mixed evidence for the Crossley et al. model and suggest that while unlearning prevents fast reacquisition, the absence of fast reacquisition does not necessarily implies that unlearning occurred.

Keywords: perceptual categorization, extinction, feedback contingency, fMRI

Introduction

Well–practiced or learned behaviors are extremely resilient. Many of us have heard the phrase “nobody ever forgets how to ride a bike”. If one learned to ride a bicycle as a child and tried again as an adult after decades of not riding, they would quickly regain the skill and feel comfortable. This resiliency of learned skills is both a blessing and a curse. On the one hand, one can pick up a musical instrument after an extended period away from playing and quickly return to their original skill level. On the other hand, maladaptive behaviors are also extremely difficult to get rid of. For example, people with substance use disorders find limited success in drug treatment facilities and relapses are common after they leave (Crossley et al., 2013).

These informal observations and maxims have been observed repeatedly in the instrumental learning literature with rodents (for a recent review, see Trask, Shipman, Green, & Bouton, 2020). In a typical experiment, the animal gradually learns to associate a behavior (e.g., pulling a lever) with a reward (e.g., a food pellet) during the *acquistion* phase. Next, the reward is removed. Pulling the lever no longer results in food reward. At this point the animal gradually reduces the frequency of behavior. This phase is called *extinction*. However, the behavior is generally not actually forgotten or *unlearned*. If the reward is re–introduced, the frequency of the behavior that was previously associated with the reward quickly jumps back to a similar frequency as in the acquisition phase. This jump is called *fast reacquisition*, and it is frequently observed during the *reacquisition* phase.

A computational model

So why is it so difficult to unlearn a skill? Crossley et al. (2013) proposed a computational model based on the procedural learning system of COVIS (Ashby, Alfonso-Reese, Turken, & Waldron, 1998) with an added context detector located in the thalamus. According to this model, when the reward structure of the environment changes (e.g., during the extinction phase) the thalamus sends a signal to the striatum that protects the category representations that have been learned by "freezing" them in place. While the previously learned category representations are frozen, new knowledge is learned without interfering with pre–existing knowledge. However, when the reward structure of the environment changes back to its original context (e.g., during the reacquisition phase), the thalamus unfreezes the category representations learned during the acquisition phase and the knowledge is available again. This accounts for the fast reacquisition observed in instrumental learning experiments.

The main prediction of the Crossley et al. (2013) model is that if one could design an experiment where the thalamus fails to detect a change in the reward context, then the category representations learned during the acqusition phase would not be protected and new knowledge could overwrite the previously learned associations during the extinction phase. This would cause unlearning and prevent fast reacquisition in the reacquisition phase. This model prediction was supported by behavioral experiments showing that random feedback during the extinction phase produced fast reacqusition (because it was easily detected), but partially–valid feedback, where feedback in 25% of the trials was contingent on behavior (with feedback in the remaining 75% of the trials being random), went undetected and did not produce fast reacquisition. Partially–valid feedback may thus be key to producing unlearning.

Alternative explanations

While Crossley et al. (2013)'s work focused on humans, substantial work has been done in the rodent literature to explain the *resurgenge* of responses after they had been extinguished. Trask, Schepers, and Bouton (2015) reviewed three possible explanations for this phenomenon: (1) response prevention, (2) behavioral momentum theory, and (3) context change. The first explanation, response prevention, suggests that during extinction the animal does not produce the behavior learned during acquisition frequently enough to be able to unlearn it (Leitenberg, Rawson, & Bath, 1970). As a result, the behavior that was learned in the acqquisition phase is still available after the extinction phase. The second explanation, based on momentum theory, suggests that behaviors with higher reinforcement rates are more resistant to change when compared to behaviors with leaner reinforcement rates (Nevin, 1974). During extinction, the reinforcer is typically not tied to behavior, so it results in a weaker association that is not sufficient to overcome what was learned in the acqusition phase. Lastly, the third explanation (context change) suggests that resurgence happens when a change in context is detected between the extinction phase and the reacquisition phase (Winterbauer & Bouton, 2010). Specifically, the animal learns to inhibit the previously learned behavior only in the extinction context. As a result, if the reacquisition context is different from the extinction context, then the behavior is no longer inhibited. Trask et al. reviewed empiricial data suggesting that the third explanation, namely a change in context, does better at accounting for resurgence in rodent behavior.

The current study

Both work with humans (Crossley et al., 2013) and rodents (Trask et al., 2015) converged on the extinction context being considered different as the critical factor for fast reacquisition. However, Crossley et al. focused on the detection of a change of context between the acquisition and extinction phases for fast reacquisition, whereas Trask et al. focused on the detection of a change of context between the extinction phase and the reacquisition phase for fast reacqusition.

In the present experiment, we replicated the Crossley et al. (2013) behavioral paradigm using a functional Magnetic Resonance Imaging (fMRI) design. Consistent with Crossley et al., we predicted that random feedback in the extinction phase would not produce unlearning, as evidenced by the presence of fast reacqusition. In contrast, partially–valid feedback in the extinction phase should yield unlearning, as evidenced by the absence of fast reacquisition. Note that this is a within–subject hypothesis tested by comparing each participant's response accuracies at the end of the acquisition phase with their response accuracies at the beginning of the reacquisition phase. If there was unlearning during the extinction phase, the accuracies at the beginning of the reacquisition phase should be lower then accuracies at the end of the acquisition phase. If the knowledge learned in the acquisition phase was preserved, then accuracies at the beginning of the reacquisition phase should be similar to those at the end of the acquisition phase (i.e., fast reacquisition).

Because both the Crossley et al. and Trask et al. explanations focused on reinforcers, we analyzed brain–related activity when the participants were processing the feedback. If the Crossley et al. model is correct, we expected to see differences in blood oxygen–level dependent (BOLD) activity between the acquisition and extinction phases in conditions where fast reacqusition is observed (e.g., when the extinction feedback is random). This is because a change in context has been detected, which protects the learned associations and prevents unlearning. If the Trask et al. (2015) explanation is correct, we expected to see differences in BOLD activity between the extinction and reacquisition phases in conditions where fast reacqusition is observed. This is because the reacquisition phase has been detected as a new context (compared to the extinction phase). As a result, the behavior that was inhibited during the extinction phase is no longer inhibited and resurges.

Most of the fMRI work in perceptual categorization so far has focused on stimulus processing; not feedback. However, previous cognitive work suggests that the main components of category learning are related to selective attention (e.g., which stimulus features are diagnostic: Ashby et al., 1998; Nosofsky, 1986; Shamloo & Hélie, 2020) and response selection (e.g., which response button is associated with which category: Cantwell, Crossley, & Ashby, 2015). As a result, we hypothesized that learning–related feedback activity would be located in the frontoparietal attention network (e.g., dorsolateral prefrontal cortex (PFC), posterior parietal cortex: Scolari, Seidl-Rathkopf, & Kastner, 2015).

Materials and methods

This experiment is based on the paradigm developped by Crossley et al. (2013). However, the present experiment lasted only one session (instead of two) and used an fMRI design. To allow participants to learn the categories in only one session, the category structures used were more easily discriminable then in Crossley et al..

Participants

Forty students from Purdue University were recruited to participate in this experiment (7 males; 33 females). Twenty participants were randomly assigned to the random (RND) condition while the remaining 20 participants were assigned to the partially–valid (PV) condition. Each participant received credits as partial completion of a course and gave written informed consent. All procedures were approved by the Purdue University Biomedical Institutional Review Board #1403014655.

Stimuli and apparatus

The stimuli were lines of various lengths and orientations backprojected on a mirror attached to a head coil using a Hyperion HD 1080p projector ($1,920 \times 1,080$ resolution). In each trial, one black line was shown in the middle of the screen. Each stimulus (line) was defined in a 2D space by a set of points ($length, orientation$) where *length* was calculated in pixels, and *orientation* (counterclockwise rotation from horizontal) was calculated in degrees.

The category structures used for both training conditions are shown in Figure 1. There were four separate categories generated using bivariate normal distributions with the randomization technique (Ashby & Gott, 1988). The categories were arbitrarily labeled with letters A–D. Only the mean length and orientation differed across categories, so that $\mu_A = (84, 128)$, $\mu_B = (128, 172)$, $\mu_C = (128, 84)$, and $\mu_D = (172, 128)$. The covariance matrix for all categories was $\Sigma = \begin{pmatrix} 60 & 0 \\ 0 & 60 \end{pmatrix}$. In each trial one set of coordinates was generated from one of the four category distributions, and the coordinates were linearly transformed as follows: $length_{disp} = 4 \times lenght_{samp}$, and $angle_{disp} = 1.5 \times angle_{samp} - 60$. These corrections to the coordinates were made to accomodate the projector's high resolution and distance. Each set of transformed coordinates was used to draw a line of the specified length and with the specified rotation angle.

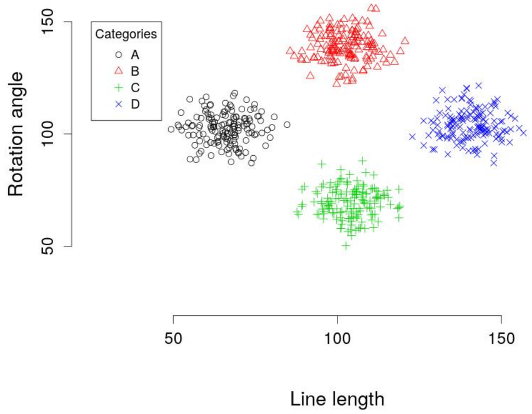

Figure 1. Category structures used in the Experiment. The *x*–axis corresponds to the length of the lines (in pixels) and the *y*–axis corresponds to the rotation angle of the lines (in degrees, counterclockwise from horizontal). Symbols denote different categories.

A single set of 600 stimuli was generated from these distributions (i.e., 150 stimuli from each category), and the stimulus set was linearly transformed so that the sample mean and covariance of each category matched the parameters of the generative distributions. The resulting set of stimulus coordinates is shown in Figure 1. The stimulus set was independently shuffled for each participant.

Stimulus presentation, feedback, and response recording were controlled and acquired using PsychoPy. Responses were produced by using two MR–compatible Celeritas button boxes (one in each hand, with three buttons on each box). The left button in the left hand corresponded to an "A" response, the right button in the left hand corresponded to the "B" response, the left button in the right hand corresponded to the "C" response, and the right button in the right hand corresponded to the "D" response. The middle button in each hand was not used.

Visual feedback was given for a correct (a green checkmark) or incorrect (a big red "X") response. If a response was too late, participants saw an hourglass. During the whole experiment, the screen background was gray.

Study design

The experiment was composed of 6 blocks of 100 trials (for a total of 600 trials), and each stimulus was shown only once. Participants were told they were taking part in a categorization experiment and that they had to assign each stimulus into either an “A”, “B”, “C”, or “D” category. The instructions were the same in both conditions and there was no mention of the different phases.

The first two blocks was the acquisiton phase and participants received valid feedback in every trial. If participants pressed the button corresponding to category “A” and the stimulus was from category “A”, they received positive feedback. Otherwise they received negative feedback. The same applied to all other categories. Blocks 3–4 was the extinction phase. During this phase, participants in the RND condition received random feedback in every trial. In other words, the feedback received was not contingent on the button they pressed; they received positive feedback in 25% of the trials and error feedback in all other trials, regardless of which button they pressed. The order of positive and error feedback was individually shuffled for each participant.

During the extinction phase, participants in the PV condition received valid feedback (contingent on their response) in 25% of the trials and random feedback (not contingent on their response) in the remaining 75% of the trials. In other words, positive or error feedback was dependent on which button they pressed in 25% of the trials but independent of which button they pressed in the other 75% of the trials. Half the invalid feedback trials showed positive feedback while the other half showed error feedback. Valid and invalid feedback trials in the PV condition were shuffled individually for each participant.

Lastly, Blocks 5–6 was the reacquisition phase. The reacquisition phase was indentical to the acquisition phase and the same for both conditions – i.e., participants in both conditions received feedback contingent on their response in all trials. Importantly, nothing indicated changes in phase in any condition. The task was presented to participants as if they were doing the same categorization task for all six blocks.

The rapid–event related design had three types of events: (1) stimulus presentation, (2) feedback presentation, and (3) crosshair. The timing of a trial [scaled in repetition time (TR), 1 TR = 720 ms] went as follows: (1) a response–terminated stimulus was presented for 3 TR. If the participant responded in less than 3 TR, the stimulus disappeared and was replaced by a blank screen for the remainder of the 3 TR. Next, feedback was presented for 1 TR. The number of blank TR between stimulus and feedback was jittered using a truncated geometric distribution ($p = 0.5$; max TR = 3) (Ashby, 2019), and the number of blank TR between feedback and the next stimulus was also jittered using a truncated geometric distribution ($p = 0.5$; max TR = 5). When more than 1 blank TR was presented between feedback in trial t and the stimulus in trial $t+1$, a fixation cross was shown for 1 TR immediately before stimulus presentation (replacing the last blank TR, so that there was always at least 1 blank TR between the feedback and the next stimulus). The crosshair was shown on an average of 48% of the trials. A schematic showing trials with positive and error feedback is shown in Figure 2.

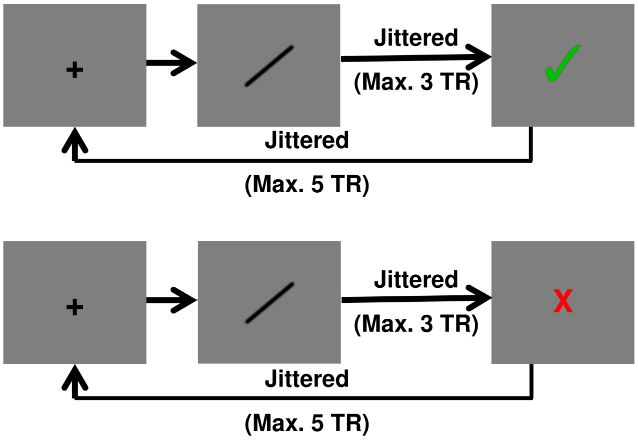

Figure 2. Experimental procedures. The top row shows an example trial with positive feedback while the bottom row shows an example trial with error feedback. The stimulus was response–terminated and presented for a maximum of 3 TR, while the feedback and crosshair (when shown) lasted 1 TR. 1 TR = 720 ms.

Neuroimaging

A rapid event–related design fMRI procedure was used to examine BOLD signal as participants categorized visual stimuli. The scanning session was conducted at the Purdue Life Science MRI Facility using a 3T Siemens Prisma scanner with a 64–channel head coil. Each block in the experiment used a separate scan. Functional runs used the lifespan HCP multiband echo–planar images (EPI) sequence (S. M. Smith et al., 2013). The sequence parameters were as follow: multiband acceleration factor: 8; TR: 720 ms; echo time (TE): 30 ms; flip angle (FA): 52°; field of view (FOV): 210 mm. Each volume consisted of 72 slices acquired parallel to the static magnetic field (z–direction) and each slice was a matrix of 104×104. The resulting voxels where 2 mm isotropic. Each functional run had a different number of TR (because of jittering) but lasted about 8 minutes.

Before the beginning of the experiment, a regular localizer was run, and after the experiment a T1–weighted MPRAGE (TR = 2,300 ms; TE = 2.98 ms; FA = 9°; 176 sagittal slices; 1.1 mm thick; 1 mm × 1 mm in–plane resolution; 256 × 256 matrix) high–resolution structural scan was run. Each scanning session lasted about 60 minutes. The experimenter talked with the participant between each scan, and the participant was allowed to take a break between each scan (but not to exit from the scanner). These manipulations were designed to minimize fatigue and monotony.

Neuroimaging analysis

Preprocessing and data analysis were conducted using FEAT (FMRI Expert Analysis Tool) version 6.00, part of FSL (`fsl.fmrib.ox.ac.uk/fsl/fslwiki`). Preprocessing was done separately on each EPI scan to reduce sources of noise and artifact, including motion correction using MCFLIRT (Jenkinson, Bannister, Brady, & Smith, 2002), BET brain extraction (S. Smith, 2002), and spatial smoothing with a FWHM of 3 mm and a high pass temporal filter with a cutoff of 100 seconds. Each functional scan (EPI) was linearly aligned with the participant's structural scan and a non–linear transformation was used for normalization to the `MNI152_1mm_brain` template. Each scan was micro–scrubbed using `fsl_motion_outliers` with default settings. This created a nuisance regressor for each TR in which motion was excessive (as automatically determined by the micro–srubbing procedure).

Univariate analyses. First, low–level analyses were performed separately on each EPI scanning block (6 per participant). Three events were defined: *Stimulus*, *Feedback*, and *Crosshair*. For the treatment blocks in the PV condition, the Feedback event was replaced by two separate events, namely *Valid Feedback* and *Invalid Feedback*. The stimulus and feedback events from trials where the participants failed to respond before the stimulus disappeared were removed from all neuroimaging analyses. Each event was modeled by a separate regressor and convolved with a double–gamma haemodynamic response function. A temporal derivative and temporal filtering were added to the design matrix. The contrast of interest was Feedback > Stimulus. In the treatment blocks of the PV condition there were two contrasts of interest: Valid Feedback > Stimulus and Invalid Feedback > Stimulus. However, no difference was detected between these two contrasts so they were averaged together in the following mid–level analyses. Crosshair was used as a nuisance regressor.

Second, the results of the low–level analyses were input into mid–level analyses to aggregate the individual blocks from the same phase. This produced three brain maps for each participant: (1) acquisition phase (average of Blocks 1 and 2), (2) extinction phase (average of Blocks 3 and 4), and (3) reacquisition phase (average of Blocks 5 and 6). Both the low– and mid–level analyses used fixed effects modeling. Next, three high–level analyses were performed using the output of the mid–level analyses as input. Analysis 1 (A1) was a within–subject analysis that compared the different phases of participants in the RND condition (i.e., Acquisition vs. Extinction, Acquisition vs. Reacquisition, and Extinction vs. Reacquisition). Analysis 2 (A2) was a within–subject analysis that compared the different phases of participants in the PV condition (same as A1 but in the other condition). Analysis 3 (A3) was a between–subject analysis that compared each phase between condition (Acquisition: RND vs. PV; Extinction: RND vs. PV; Reacquisition: RND vs. PV). The high–level analyses used random effects modeling (FLAME 1+2) with a threshold value of $Z > 3.71902$ and cluster–size correction of $p < .05$.

Multivariate pattern analyses. A multivariate pattern analysis (MVPA) was performed to investigate if patterns of activity in the inferior parietal lobules (IPL) and superior parietal lobules (SPL) could be used to classify the various phases and conditions in the experiment. While the univariate analyses described above tested for the hypothesis that individual voxels behave differently in the experimental phases and conditions, the MVPA tested instead for the hypothesis that distributed patterns of activity differed between the experiment phases and conditions. Given that complex cognitive functions are unlikely to be supported by individual voxels, but instead a distributed pattern of activities, the MVPA may provide a better test of our hypotheses.

The IPL and SPL were selected as seed regions of interests (ROI) based on our hypothesis about the important role of posterior parietal cortex in learning–related feedback processing and the results from the univariate analyses. First, we created anatomical masks of the ROIs using the Harvard–Oxford Structural Atlas applied to the `MNI152_1mm_brain` template. The IPL mask was created by adding the supramarginal gyrus (anterior), supramarginal gyrus (posterior), and the angular gyrus. The SPL mask was created by taking the superior parietal lobule. Both masks were bilateral and thresholded at 50. These masks were applied to the output of each participant's mid–level univariate analyses. As a result, the inputs to the MVPA were one IPL brain map of z–values for each participant in each phase of the experiment, and one SPL brain map of z–values for each participant in each phase of the experiment.

For each analysis, we used a linear support vector machine (SVM) with leave–one–out cross–validation. In leave–one–out cross–validation, the SVM is trained using all the brain maps except for one, and the resulting trained model is then used to classify the brain map that was left out at training. This process is repeated until each brain map has been excluded once, and prediction accuracies are then averaged.

The following analyses were performed: (1) predicting phase for each brain map in the RND condition; (2) predicting phase for each brain map in the PV condition; and (3) predicting condition using brain maps from individual phases. Each individual SVM was used to perform a binary classification, so chance performance for each SVM was 50% correct classification. We used a binomial distribution with Bonferroni correction for multiple–testing to find a classification threshold that was statistically significant above chance ($p < .05$). Classification accuracy above 67.5% was considered statistically significant above chance. All MVPA were run using in–house code written in Matlab.

Results

Behavioral results

Participants in both conditions learned the categories and improved their response accuracy in the acquisition phase from an average of 27% correct in the first 50 trials to 43.2% correct in the last 50 trials of that phase. The full learning curves are shown in Figure 3 (left panel). Because fast reacquisition is most clearly seen at the beginning of the reacquisition phase (Crossley et al., 2013), the critical test to determine if the modified paradigm was able to eliminate fast reacquisition is a within–subject comparison between the last 50 trials of the acquisition phase and the first 50 trials of the reacquisition phase. This comparison is shown in the right panel of Figure 3. Finding a significant reduction in accuracy between the end of the acquisition phase and the beginning of the reacquisition phase would provide evidence that fast reacquisition was eliminated. As predicted by the explanations reviewed in the *Introduction*, there was no statistical difference in accuracies between the end of the acquisition phase and the beginning of the reacquisition phase in the RND condition [$t(19) = 0.9, p = .38$, $BF_{01} = 3.01$]. The mean accuracy difference in the RND condition was 0.03. The Bayes factor indicates that the null hypothesis (i.e., the absence of unlearning) was three times more likely then the alternative hypothesis. This is consistent with the presence of fast reacquisition in the RND condition: participants quickly picked up where they left off at the beginning of the reacquisition phase. However, this accuracy difference was statistically significant in the PV condition [$t(19) = 2.38, p < .05$, $BF_{10} = 2.21$]. The mean accuracy difference in the PV condition was 0.07. The Bayes factor indicates that the alternative hypothesis (i.e., the presence of unlearning) was a over twice as likely then the null hypothesis. This suggest that participants needed to relearn the categories. These results replicated the elimination of fast reacquisition in the partially–valid feedback condition first observed by Crossley et al. (2013).

Neuroimaging results

Within–subject analyses. Analysis A1 explored the effect of phase in the RND condition. The goal of this analysis was to determine which brain areas process the feedback differently in the various phases of the experiment. As a reminder, no instruction was provided to the participants about experiment phases: the experiment was presented as a continuous six block category learning experiment. In total, six contrasts were computed: (1) Acquisiton > Extinction, (2) Acquisition > Reacquisition, (3) Extinction > Reacquisition, (4) Acquisiton < Extinction, (5) Acquisition < Reacquisition, and (6) Extinction < Reacquisition. Of these six contrasts, only Acquisition > Reacquisition (Contrast 2) yielded statistically significant clusters. The cluster locations are listed in Table 1 and shown in Figure 4.

As can be seen, most of the active clusters were located in the bilateral SPL and occipital cortices, with a small amount of activity also located in the cerebellum and the right IPL. Both the SPL and IPL are part of the frontoparietal network (Scolari et al., 2015), and the SPL (where the larger clusters are located) has been shown to play an important role in top–down attentional orienting (Shomstein, 2012). Attentional orienting is a critical aspect of category learning (Hélie, Shamloo, & Ell, 2017; Shamloo & Hélie, 2020). Because the behavioral results were consistent with the presence of fast reacquisition in the RND condition, there may have been limited learning during the reacquisition phase, so most of the attention learning likely happened during the acquisition phase.

The second within–subject Analysis (A2) explored the effect of phase in the PV condition. The goal and contrasts were the same as in Analysis A1. Three within–subject contrasts yielded statistically significant clusters in the PV condition: Acquisition > Extinction (Contrast 1), Acquisition > Reacquisition (Contrast 2), and Extinction < Reacquisition (Contrast 6). The cluster coordinates for these three contrasts are listed in Table 2. The clusters for Acquisition > Extinction (red/yellow) and Extinction < Reacquisition (blue) are also shown in Figure 5. Because all the clusters for the Acquisition > Reacquisition contrast were located in the occipital lobe, and we did not have any strong hypothesis about the role of these regions in the current task, these clusters are not shown in the Figure.

As can been seen in the middle and bottom rows of Figure 5, both the acquisition and reacquisition phases showed clusters located in the left IPL (part of the frontoparietal network) where BOLD signal was higher compared to the extinction phase. The acquisition phase also showed caudate activity when compared to the extinction phase (top row of Figure 5). The IPL has been shown to be related to rule switching (Philipp, Weidner, Koch, & Fink, 2013) directed by a top–down attentional signal (Shomstein, 2012). This is consistent with participants switching between categorization rules in the acquisition and reacquisition phases (Hélie, Shamloo, Zhang, & Ell, 2021). The caudate activity found in the acqusitiion phase is consistent with the hypothesis–testing phase when initially acquiring categorization rules (Hélie, Roeder, & Ashby, 2010).

Between–subject analyses. Analysis A3 compared the two conditions (i.e., RND vs. PV) within each phase. In total, six contrasts were computed: (7) Acquisition: RND > PV, (8) Acquisition: RND < PV, (9) Extinction: RND > PV, (10) Extinction: RND < PV, (11) Reacquisition: RND > PV,

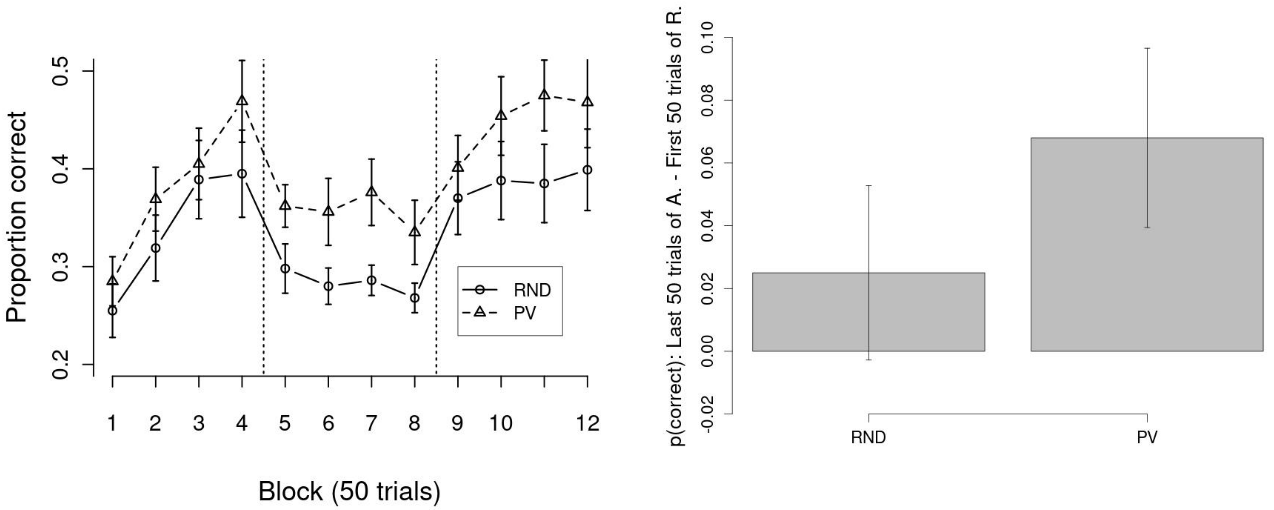

Figure 3. Left. Mean accuracy for each block in each condition. *Right.* Mean accuracy difference between the last 50 trials of the acquisition phase and the first 50 trials of the reacquisition phase. Error bars in both panels are between–subject standard error of the mean. A = acquisition phase; R = reacquisition phase.

Table 1

Analysis A1 (RND): Acquisition > Reacquisition

				Coordinates			
Cluster	Size	*p*	*Max*(*Z*)	*x*	*y*	*z*	Brain regions
1	4,663	< .0001	7.23	15	-81	6	R. Intracalcarine cortex
2	391	< .0001	5.54	17	-65	55	R. Superior parietal lobule (posterior)
3	272	< .0001	5.10	-22	-58	1	L. Lingual gyrus
4	221	< .0001	4.89	-10	-76	49	L. Superior parietal lobule (posterior)
5	173	.0003	4.75	-21	-85	-14	L. Occipital fusiform gyrus
6	155	.0006	4.78	-25	-76	-14	L. Occipital fusiform gyrus
7	150	.0007	4.73	26	-61	54	R. Superior parietal lobule (anterior)
8	136	.0014	4.61	-28	-69	53	L. Superior parietal lobule (anterior)
9	118	.0034	4.89	12	-79	44	R. Precuneus
10	83	.0224	4.67	41	-58	-24	R. Cerebellum
11	75	.0356	4.67	41	-38	67	R. Postcentral gyrus
12	72	.0425	5.31	-27	-70	-23	L. Cerebellum
13	70	.0479	4.47	58	-38	53	R. Inferior parietal lobule

and (12) Reacquisition: RND < PV. Only two of these contrasts yielded statistically significant clusters, namely (Contrast 10) (Extinction: RND < PV) and (Contrast 12) (Reacquisition: RND < PV). The fact that no difference was found between the conditions during the Acquisition phase (Contrasts 7 and 8) served as a sanity check in that no manipulation had been introduced yet, so participants in both conditions were doing the same task and had the same experience so far in the experiment. We found no evidence that participants' brains processed the feedback differently in the two conditions during that phase.

The cluster coordinates for Extinction: RND < PV are listed in Table 3 and shown in Figure 6. Because the first cluster is large (> 30,000 voxels), the peaks of this cluster are listed separately in Table 4. As can be seen, this contrast yielded by far the most widespread BOLD activity, with several clusters located in the frontal and parietal lobes. Smaller clusters of activity were also found in the occipital and temporal lobes.

First, similar to the results of Analyses A1 and A2, the parietal lobe showed bilateral activity in both the IPL and SPL. These brain areas were more active during extinction in the PV condition when compared to the RND condition. This is consistent with the top–down attentional roles of the

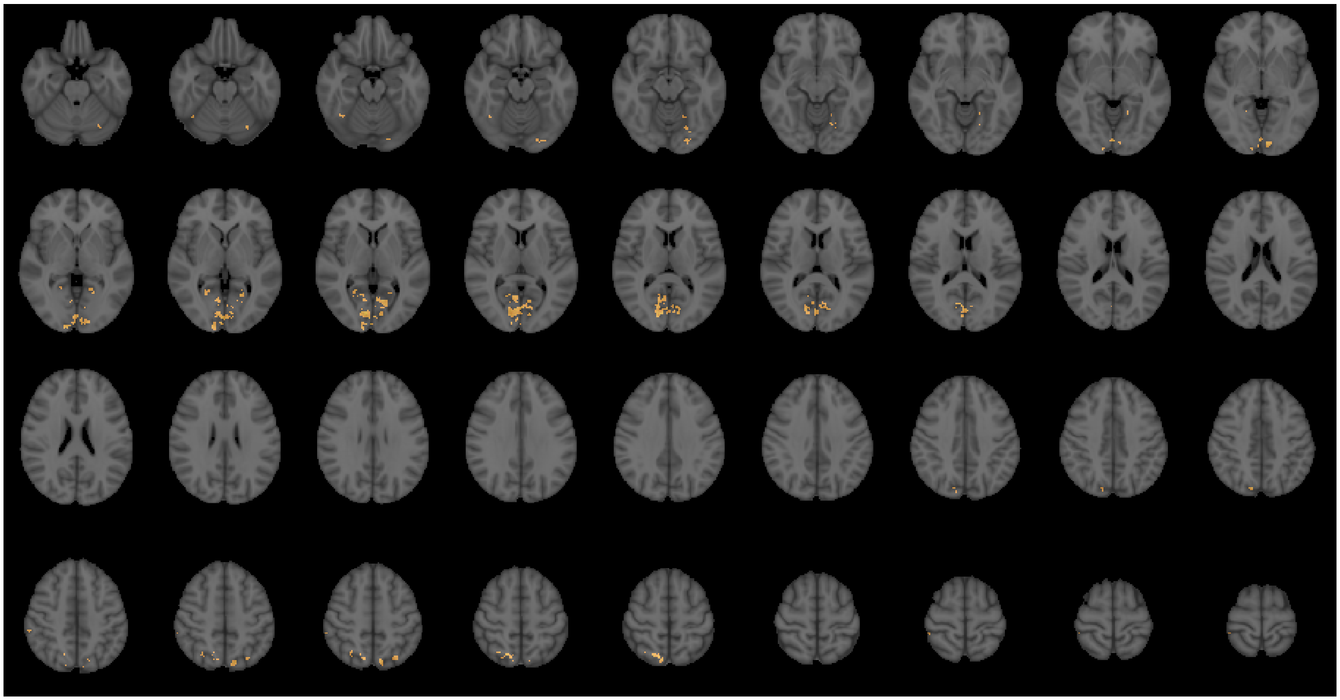

Figure 4. BOLD clusters for Analysis A1 (RND): Acquisition > Reacquisition. The slices shown range from $z = -25$ to $z = 68$ from left to right and top to bottom by jumps of 2.6. Cluster coordinates are listed in Table 1.

IPL and SPL that has been noted previously. Fast reacquisition was eliminated in the PV condition. If the absence of fast reacquisition was caused by unlearning (Crossley et al., 2013), participants may have continued trying to learn or adjust their categorical knowledge during the extinction phase by updating their attentional control to the different stimulus features. In contrast, behavioral results were consistent with the presence of fast reacquisition in the RND condition, suggesting that participants may have disengaged from the task and not used the feedback provided to update their categorical knowledge.

Second, a number of clusters of BOLD activity were located in the frontal lobes. Note that we did not observe frontal activity in the within–subject analyses (A1 and A2), but this constitutes the other half of the frontoparietal network (Petersen & Posner, 2012; Vossel, Geng, & Fink, 2014). The observed activity was bilateral and included both areas of the ventral and dorsal PFC. The PFC plays an important role in category learning and working memory (WM) (Ashby, Ell, Valentin, & Casale, 2005). These results are again consistent with participants in the PV condition trying to use feedback to update their category representations during extinction. In contrast, participants in the RND condition did not seem to process feedback as much, which may explain why their categorical knowledge remained mostly intact at the end of the extinction block.

Third, Table 3 also shows one cluster (15) located in the right temporal gyrus. The only cluster found in Contrast 12 (Reacquisition: RND < PV) was also located in the right temporal gyrus ($size = 132, p = .0062, Max(Z) = 5.26, x = 68, y = -19, z = -15$). Similar to occipital cortex, we did not have any strong *a priori* hypothesis about the role of the temporal lobe in this task. The cluster in Contrast 10 appears to be located in areas typically related to vision while the cluster in Contrast 15 is located in areas typically related to the auditory systems. These results were included for completeness but need to be interpreted with care since they did not test any hypothesis that we had *a priori*.

MVPA. The MVPA were run to determine if z–values from the univariate analyses located in the IPL and SPL could be used to classify brain maps into the correct condition (i.e., RND vs. PV) or experimental phase (i.e., Acquisition vs. Extinction vs. Reacquisition). Table 5 shows the proportion of phases that were correctly predicted using data from the IPL and SPL. As can be seen, both the IPL and SPL could classify brain maps comparing the extinction and reacquisition phases accurately. This suggests that both these brain areas process the feedback differently when it becomes reliable again in the reacquisition phase after the extinction phase. This result is consistent with the context change explanation of resurgence from the rodent literaure (Trask et al., 2015). In addition, the IPL was able to distinguish between the acquisition and extinction phases, but only in the RND condition. This result is consistent with the Crossley et al. (2013) model suggesting that participants could detect a change in context between these phases in the RND con-

Table 2
Analysis A2: PV condition

Cluster	Size	p	$Max(Z)$	Coordinates x	y	z	Brain regions
Acquisition > Extinction							
1	168	.0004	4.62	-40	-68	50	L. Inferior parietal lobule
2	90	.0181	4.68	18	-12	26	R. Caudate
3	76	.0394	4.69	-11	-73	-8	L. Lingual gyrus
Acquisition > Reacquisition							
1	3,579	< .0001	5.72	-14	-73	11	L. Intracalcarine cortex
2	679	< .0001	5.32	11	-100	-1	R. Lingual gyrus / Occipital pole
3	196	.0002	4.94	-8	-85	0	L. Intracalcarine cortex
4	170	.0004	4.43	33	-91	-6	R. Lateral occipital cortex, inferior division
5	131	.0023	5.41	-30	-87	-19	L. Occipital fusiform gyrus
Extinction < Reacquisition							
1	111	.0060	4.80	-48	-71	41	L. Inferior parietal lobule

dition but not the PV condition. Lastly, the IPL could also distinguish between the acquisition and reacquisition phases, but only in the PV condition. Earlier explanations did not directly address the relationship between the acquisition and reacquisition phases but the fact that accurate classification was only achieved in the PV condition is noteworthy (we come back to this result in the *Discussion* section). Lastly, Table 6 shows the IPL's and SPL's ability to classify brain maps in the two conditions within each phase. As can be seen, the MVPA was unable to predict condition in any of the phase.

Discussion

This article explored how manipulations of feedback contingencies could affect the ability to unlearn a skill. Crossley et al. (2013) previously showed that using partially–valid feedback in an extinction paradigm could eliminate fast reacquisition, which they interpreted as evidence of unlearning of the category representations learned during the acquisition phase. We reported results from a fMRI experiment that was closely inspired by the work of Crossley et al. (2013). The behavioral results replicated those found by Crossley et al. in that using partially–valid feedback during the extinction phase eliminated fast reacqusition whereas using random feedback during the extinction phase was consistent with the presence of fast reacquisition.

The main novelty of the new experiment was the inclusion of the fMRI component. As predicted, feedback processing yielded a number of significant clusters in posterior parietal cortex (mostly in the IPL and SPL) and the PFC. This result was strongest in univariate analysis A3, where the PV condition showed much stronger activation in the whole frontoparietal attentional network compared to the RND condition during the extinction phase. However, the main goal of the experiment was to determine if the presence of fast reacquisition was caused by a change of context between the extinction and reacquisition phases (as suggested by the rodent literature: Trask et al., 2015) or a change of context between the acquisition and extinction phases (Crossley et al., 2013). We found mixed results for both mechanisms.

The univariate analysis A2 showed more IPL and caudate activity during the acquisition phase compared to the extinction phase in the PV condition. This result is problematic for the Crossley et al. model, since participants in that condition should have failed to detect a change in context and continue processing feedback to update their category representations during extinction (thus producing unlearning). Second, univariate analysis A2 also showed more IPL activity in the reacquisition phase compared to the extinction phase in the PV condition. This result is problematic for the Trask et al. explanation: the category representations learned during the acquisition phase should have been inhibited in the extinction context only, so detecting the context change in the reacquisition phase should lead to fast reacquisition (which was not observed in the PV condition).

The univariate results described above were further informed by results from the MVPA. First, the IPL was able to classify brain maps from the RND condition into the acquisition or extinction phase; this classification failed in the PV condition. This is consistent with the Crossley et al. (2013)

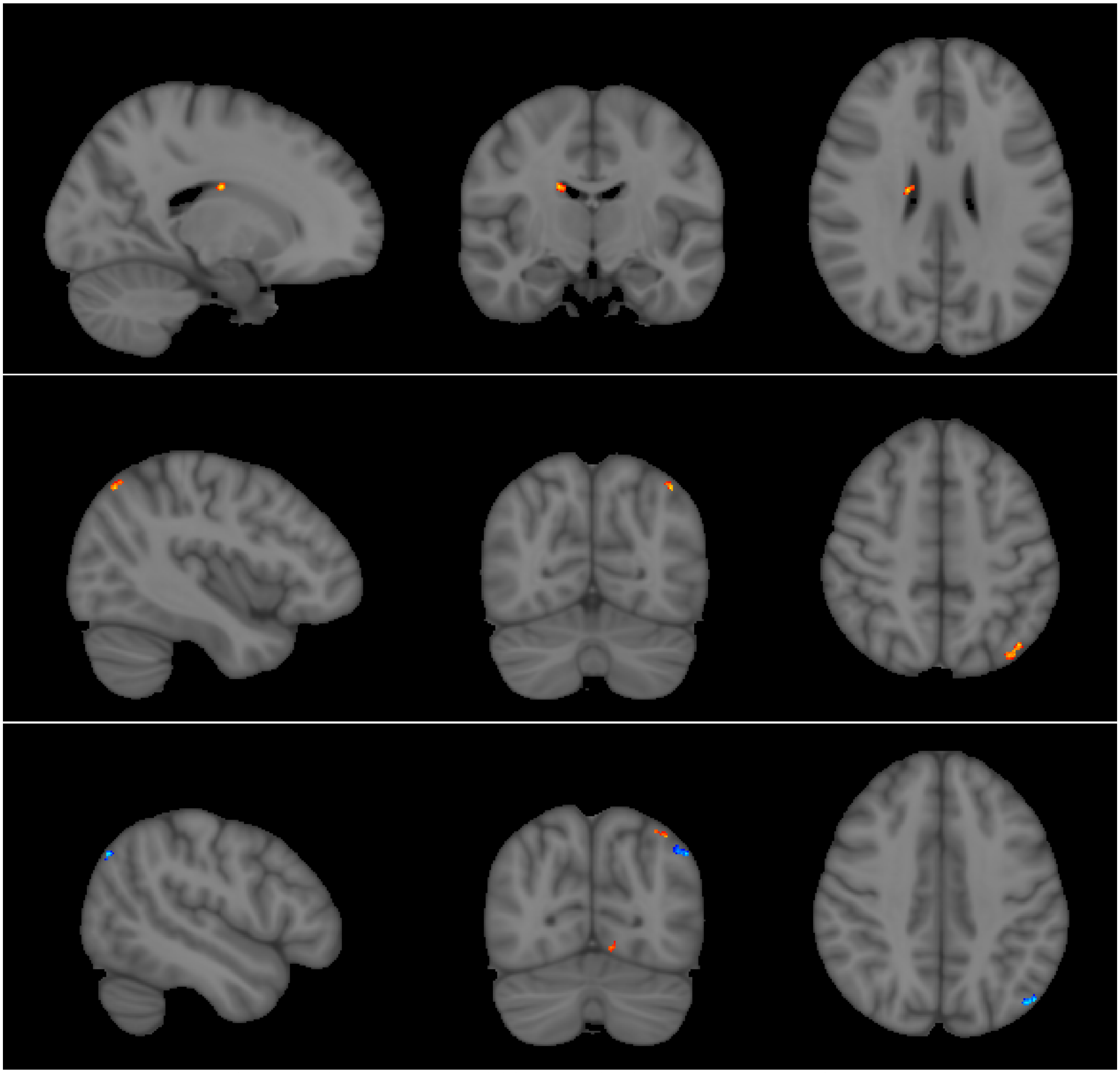

Figure 5. BOLD clusters for Analysis A2 (PV): Acquisition > Extinction (red/yellow) and for Analysis A2 (PV): Extinction < Reacquisition (blue). The first row shows caudate activity while the middle and bottom rows show IPL activity. Each row is centered on the *Max(Z)* coordinates for their respective cluster as listed in Table 2.

model which suggests that the change of context is only detected in the RND condition. According to this model, the failure in detecting the change of context in the PV condition produces unlearning. Second, the MVPA showed that both the IPL and SPL could classify brain maps in the extinction or reacquisition phase in both conditions. This is consistent with Trask et al. (2015)'s explanation that the extinction and reacquisition phases are treated as different context. The accurate classification in the RND condition is consistent with the presence of fast reacquisition (or resurgence) in that condition, but the accurate classification in the PV condition is inconsistent with the absence of fast reacquisition in that condition. Detecting the change in context in the PV condition should have led to fast reacquisition.

One intriguing result of the MVPA is that the IPL was able to classify brain maps in the acquisition or reacquisition phases, but only in the PV condition. While the Trask et al. (2015) explanation does not directly address the relation-

Table 3
Analysis A3: Extinction: RND < PV

Cluster	Size	p	$Max(Z)$	Coordinates x	y	z	Brain regions
1	38,292	< .0001	8.72	-50	-39	59	See Table 4
2	810	< .0001	6.93	-54	12	32	L. Precentral / Inferior frontal (pars opercularis) gyri
3	609	< .0001	7.26	-29	-5	69	L. Superior frontal / precentral gyri
4	513	< .0001	6.94	-14	-77	40	L. Precuneus cortex
5	360	< .0001	6.07	-44	-70	3	L. Lateral occipital cortex, inferior division
6	296	< .0001	5.14	52	-67	15	R. Inferior parietal lobule
7	283	< .0001	5.79	64	-27	24	R. Supramarginal gyrus, anterior division / Inferior parietal lobule
8	270	< .0001	7.30	31	-4	66	R. Superior frontal gyrus
9	236	.0002	6.30	-42	-77	17	L. Inferior parietal lobule
10	230	.0002	4.84	0	-37	52	Superior parietal lobule
11	215	.0003	6.04	15	-32	41	R. Superior parietal lobule
12	192	.0007	5.33	47	31	18	R. Inferior frontal gyrus, pars triangularis
13	191	.0007	4.96	19	-55	-14	R. Lingual gyrus / cerebellum
14	157	.0023	4.78	-52	23	36	L. Middle Frontal Gyrus
15	145	.0037	4.75	51	-60	-7	R. Inferior temporal gyrus, temporooccipital part
16	131	.0065	5.30	-14	-35	45	L. Superior parietal lobule
17	119	.0107	4.84	-8	-26	44	L. Cingulate gyrus, posterior division
18	108	.0172	5.38	-39	-3	16	L. Central opercular cortex
19	106	.0188	6.28	45	-76	16	R. Lateral occipital cortex, superior division
20	100	.0246	4.43	43	-39	62	R. Superior parietal lobule
21	100	.0246	5.18	38	-38	58	R. Postcentral gyrus
22	97	.0282	4.73	-33	36	44	L. Middle Frontal Gyrus
23	96	.0295	6.13	1	-77	10	R. Supracalcarine / intracalcarine cortex
24	96	.0295	4.46	16	-48	-48	R. Cerebellum
25	86	.0468	4.88	38	-43	-28	R. Cerebellum

Note. Local maxima for Cluster 1 are shown in Table 4.

ship between the acquisition and reacquisition phases, the Crossley et al. model implicitely assumes that the reacqusition phase context is sufficiently similar to the acquisition phase context to bring back the earlier learned associations (hence the fast reacquisition). The fact that reacquisition is treated differently then acquisition by the IPL in the PV condition could show that the categorization problem in the reacquisition phase is treated as a new problem from the acquisition phase instead of being a return to the original categorization problem. This would be expected if the information learned during the acquisition phase has been unlearned. However, another possibility is that fast reacquisition was not observed in the PV condition not because unlearning occured, but instead because the reacquisition context failed to be identified as being the same as the acquisition context. The present experiment was not designed to distinguish between these two possible interpretations, but future researh could directly address this issue by explicitly cueing the context in the various phases of the experiment (e.g., by associating phases with background colors).

Overall, the present research found evidence for the importance of changes in context both between the acquisition and extinction phases, as well as between the extinction and reacquisition phases. The key to disentangling the effects of these two changes in context may be to treat unlearning and fast reacqusition as separate concept: the presence of unlearning necessarily prevents fast reacquisition (because the knowledge has been “erased”), but the absence of fast reacquisition is not necessarily indicative of unlearning. More research is needed to establish a more stringent test of unlearning using an observed phenomenon instead of the absence of a phenomenon.

Competing interest

The author declares that he has no financial interests.

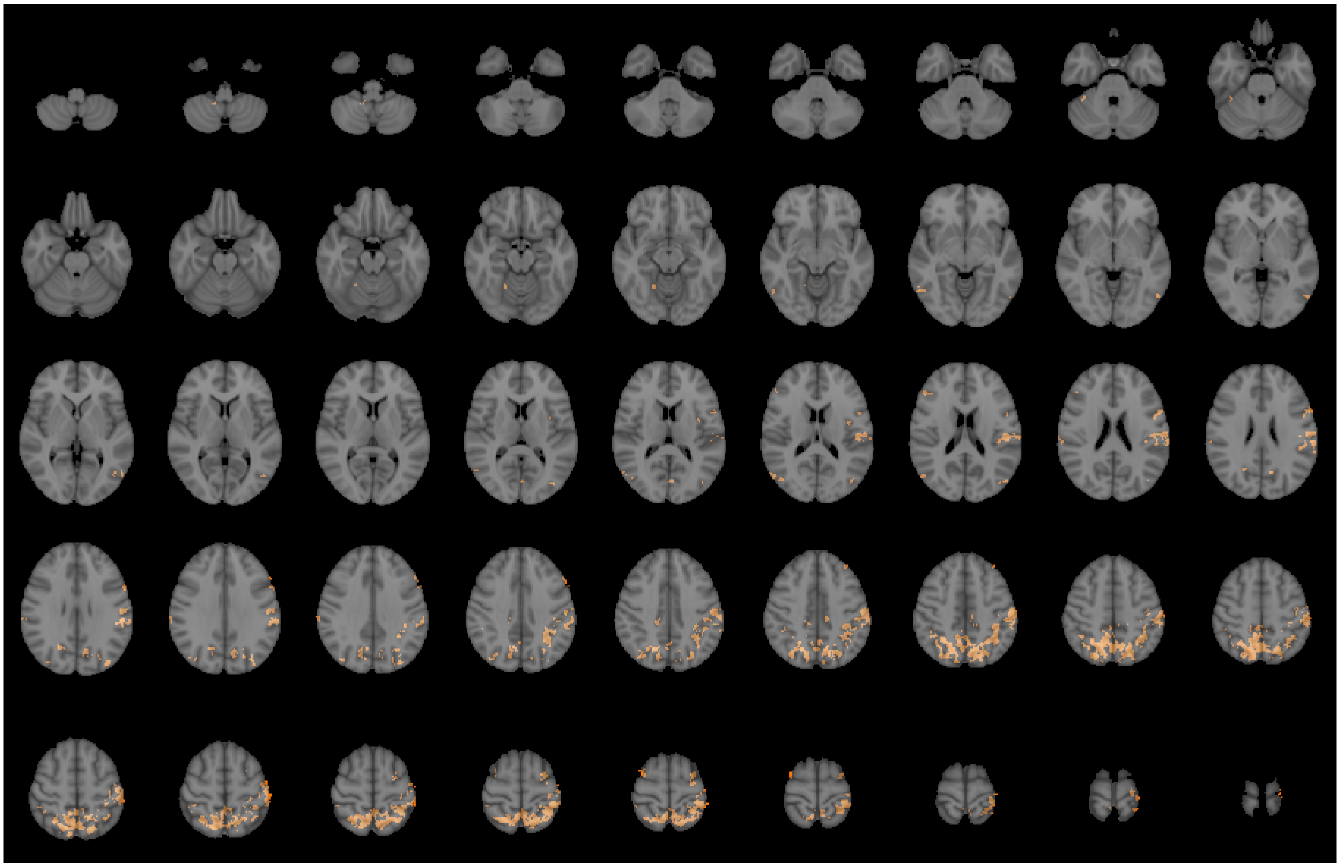

Figure 6. BOLD clusters for Analysis A3 (Extinction: RND < PV). The slices are the same as in Figure 4. Cluster coordinates are listed in Tables 3 and 4.

Table 4

Local maxima in Cluster 1 from Table 3

Maximum	*Max*(*Z*)	Coordinates *x*	*y*	*z*	Brain regions
1	8.72	-50	-39	59	L. Postcentral gyrus
2	7.92	-58	-21	42	L. Postcentral gyrus
3	7.87	-25	-72	44	L. Lateral occipital cortex, superior division
4	7.80	-56	-22	42	L. Postcentral gyrus
5	7.78	-24	-73	47	L. Lateral occipital cortex, superior division
6	7.48	-25	-71	46	L. Lateral occipital cortex, superior division

Data Availability

The data and materials for the experiment are available by contacting the corresponding author.

Acknowledgements

Correspondence should be addressed to Dr. Sébastien Hélie, `shelie@purdue.edu`. This research was supported in part by NSF grant #1349677-BCS. The author would like to thank Drs. Farzin Shamloo and Madison J. Adkins for help with data collection, as well as Corey Nack and Moon Sun Kang for help with data analysis. We would also like to thank Drs. Yu–Chin Chiu and Illia Kuznietsov for comments on an earlier draft of this manuscript.

References

Ashby, F. G. (2019). *Statistical Analysis of fMRI Data* (2nd ed.). Cambridge, MA: MIT Press.

Ashby, F. G., Alfonso-Reese, L. A., Turken, A. U., & Waldron, E. M. (1998). A neuropsychological theory of multiple systems in category learning. *Psychological Review*, *105*(3), 442–481.

Table 5

MVPA results: Proportion of correct phase predictions

	SPL			IPL		
Condition	A vs. E	A vs. R	E vs. R	A vs. E	A vs. R	E vs. R
RND	0.625	0.550	0.700*	0.800*	0.550	0.725*
PV	0.475	0.500	0.675*	0.575	0.775*	0.725*

Note. A = Aquisition; E = Extinction; R = Reacquisition. * denotes a proportion of correct predictions that is statistically better then chance accuracy ($p < .05$).

Table 6

MVPA results: Proportion of correct predictions of participants' condition

Condition	Aquisition	Extinction	Reacquisition
IPL	0.525	0.225	0.475
SPL	0.475	0.550	0.625

Ashby, F. G., Ell, S. W., Valentin, V. V., & Casale, M. B. (2005). FROST: A distributed neurocomputational model of working memory maintenance. *Journal of Cognitive Neuroscience*, *17*(11), 1728–1743.

Ashby, F. G., & Gott, R. E. (1988). Decision rules in the perception and categorization of multidimensional stimuli. *Journal of Experimental Psychology: Learning, Memory, and Cognition*, *14*, 33–53.

Cantwell, G., Crossley, M. J., & Ashby, F. G. (2015). Multiple stages of learning in perceptual categorization: evidence and neurocomputational theory. *Psychonomic Bulletin & Review*, *22*, 1598–1613. Retrieved from `http://link.springer.com/10.3758/s13423-015-0827-2` doi: 10.3758/s13423-015-0827-2

Crossley, M. J., Ashby, F. G., & Maddox, W. T. (2013). Erasing the engram: The unlearning of procedural skills. *Journal of Experimental Psychology: General*, *142*(3), 710.

Hélie, S., Roeder, J. L., & Ashby, F. G. (2010, oct). Evidence for cortical automaticity in rule-based categorization. *Journal of Neuroscience*, *30*(42), 14225–14234. doi: 10.1523/JNEUROSCI.2393-10.2010

Hélie, S., Shamloo, F., & Ell, S. W. (2017). The effect of training methodology on knowledge representation in categorization. *PLOS ONE*, *12*, e0183904.

Hélie, S., Shamloo, F., Zhang, H., & Ell, S. W. (2021). The impact of training methodology and representation on rule–based categorization: An fMRI study. *Cognitive, Affective, & Behavioral Neuroscience*, *21*, 717–735.

Jenkinson, M., Bannister, P., Brady, M., & Smith, S. (2002). Improved optimisation for the robust and accurate linear registration and motion correction of brain images. *NeuroImage*, *17*, 825–841.

Leitenberg, H., Rawson, R. A., & Bath, K. (1970). Reinforcement of competing behavior during extinction. *Science*, *169*, 301–303.

Nevin, J. A. (1974). Response strength in multiple schedules. *Journal of the Experimental Analysis of Behavior*, *21*, 389–408.

Nosofsky, R. M. (1986). Attention, similarity, and the identification–categorization relationship. *Journal of Experimental Psychology: General*, *115*, 39–57.

Petersen, S. E., & Posner, M. I. (2012, jan). The attention system of the human brain: 20 years after. *Annual review of neuroscience*, *35*, 73–89.

Philipp, A. M., Weidner, R., Koch, I., & Fink, G. R. (2013). Differential roles of inferior frontal and inferior parietal cortex in task switching: Evidence from stimulus-categorization switching and response-modality switching. *Human Brain Mapping*, *34*(8), 1910–1920. doi: 10.1002/hbm.22036

Scolari, M., Seidl-Rathkopf, K. N., & Kastner, S. (2015). Functions of the human frontoparietal attention network: Evidence from neuroimaging. *Current Opinion in Behavioral Sciences*, *1*, 32–39. Retrieved from `http://dx.doi.org/10.1016/j.cobeha.2014.08.003` doi: 10.1016/j.cobeha.2014.08.003

Shamloo, F., & Hélie, S. (2020). A study of individual differences in categorization with redundancy. *Journal of Mathematical Psychology*, *99*, 102467.

Shomstein, S. (2012). Cognitive functions of the posterior parietal cortex: Top-down and bottom-up attentional control. *Frontiers in Integrative Neuroscience*, *6*(JULY 2012), 1–7. doi: 10.3389/fnint.2012.00038

Smith, S. (2002). Fast robust automated brain extraction. *Human Brain Mapping*, *17*, 143–155.

Smith, S. M., Beckmann, C. F., Andersson, J., Auerbach, E. J., Bijsterbosch, J., Douaud, G., … for the WU-Minn HCP Consortium (2013). Resting–state fMRI in the Human Connectome Project. *NeuroImage*, *80*, 144–168.

Trask, S., Schepers, S. T., & Bouton, M. E. (2015). Context change explains resurgence after the extinction of operant behavior. *Revista Mexicana de Analisis de la Conducta*, *41*(2), 187–210. doi: 10.5514/rmac.v41.i2.63772

Trask, S., Shipman, M. L., Green, J. T., & Bouton, M. E. (2020). Some factors that restore goal-direction to a habitual behavior. *Neurobiology of Learning and Memory*, *169*(September 2019), 107161. Retrieved from `https://doi.org/10.1016/j.nlm.2020.107161` doi: 10.1016/j.nlm.2020.107161

Vossel, S., Geng, J. J., & Fink, G. R. (2014). Dorsal and ventral attention systems: Distinct neural circuits but collaborative roles. *Neuroscientist*, *20*(2), 150–159. doi: 10.1177/1073858413494269

Winterbauer, N. E., & Bouton, M. E. (2010). Mechanisms of resurgence of an extinguished instrumental behavior. *Journal of Experimental Psychology: Animal Behavior Processes*, *36*, 343–

353.